Closed-Loop Control Tests for Vertical Fin Buffeting Alleviation Using Strain Actuation

F. Nitzsche*
Carleton University, Ottawa, Ontario K1S 5B6, Canada
D. G. Zimcik†
National Research Council of Canada, Ottawa, Ontario K1A 0R6, Canada
T. G. Ryall‡
Aeronautical and Maritime Research Laboratory, Melbourne, Victoria 3001, Australia
R. W. Moses§
NASA Langley Research Center, Hampton, Virginia 23681-2199
and
D. A. Henderson¶
U.S. Air Force Research Laboratory, Wright–Patterson Air Force Base, Ohio, 45433-7006

Introduction

THE F/A-18, known in Canada as the CF-188, is often subjected to high-intensity buffet loads that produce accelerations in excess of 450 g at the tip of the vertical fin during maneuvers at high angles of attack. Previous investigations were able to demonstrate that the first and the second natural modes of the vertical fin at approximately 17 Hz (bending) and 43 Hz (coupled bending torsion), respectively, contribute most significantly to the buffeting phenomenon.[1–4] The resulting loads substantially contribute to the fatigue of the tail structure, increasing the maintenance costs of the fighter.

The overall approach is to develop an active control system that includes strain actuation using piezoelectric elements. However, the ability of the piezoelectric actuators to achieve control authority under the large aerodynamic buffet loads in a full-scaled aircraft needs to be demonstrated. The closed-loop tests of the proposed active control system were carried out in the International Follow-on Structural Test Project rig in Melbourne, Australia, in the period between 12 January and 13 February 1998. These tests represented an important milestone in the development of adaptive structures systems with application to aeroelastic problems because they were the first tests performed on a full-scale airframe to achieve buffeting alleviation. The present work reports the control design strategy and the results obtained in the closed-loop tests. The hardware was configured to accept a multi-input/multi-output (MIMO) feedback control system with up to two inputs (consisting of a choice among several strain gauges and accelerometers distributed over the surface of the vertical fin to measure the performance of the system) and two outputs that drive two groups of piezoelectric actuators attached to both sides of the structure skin.

Some earlier studies incorporating active control techniques to suppress aerodynamic buffeting focused on the classical aeroelastic approach, where the rudder was the actuation device.[5] Adaptive structures provide an attractive solution to the problem.[6,7] Besides having higher frequency bandwidths, piezoelectric actuators allow for the development of sensor and actuator arrangements that are able to perform approximately independent modal state control, greatly improving the realization of a more efficient and robust closed-loop aeroelastic system.

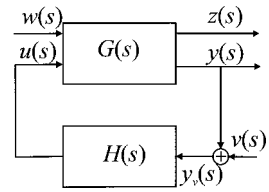

Fig. 1 Output feedback active control system (disturbance rejection).

Control Synthesis

Figure 1 shows the schematics of the closed-loop, output feedback control system analyzed. The buffeting pressure acting on the fin was treated as a disturbance, $\boldsymbol{w}(s)$, of stochastic nature. The other input vector $\boldsymbol{u}(s)$ is due to the action of the two actuator groups, which were patched to the structure to reproduce as closely as possible the strain distribution associated with each one of the first two aeroelastic modes. Hence, each group had more control authority over one specific mode of the structure. Two vectors, $\boldsymbol{z}(s)$ and $\boldsymbol{y}(s)$ defined the system output: $\boldsymbol{z}(s)$ is the signal produced by the sensor monitored for performance (normally the strain gauge located at the critical point for fatigue at the fin root), and $\boldsymbol{y}(s)$ is the signal originating from the two sensors used for the feedback control. Here $v(s)$ is the transducer noise, $G(s)$ is the feedforward (plant) transfer function, and $H(s)$ is the feedback (controller) transfer function.

The frequency-domain transfer function representation of the MIMO system presented in Fig. 1 is

$$\begin{Bmatrix} \boldsymbol{y}_v(s) \\ \boldsymbol{z}(s) \end{Bmatrix} = \begin{bmatrix} G_{11}(s) & G_{12}(s) \\ G_{21}(s) & G_{22}(s) \end{bmatrix} \begin{Bmatrix} \boldsymbol{u}(s) \\ \boldsymbol{w}(s) \end{Bmatrix} \tag{1}$$

For the open-loop case, Eq. (1) gives

$$\boldsymbol{z}(s) = G_{22}(s)\boldsymbol{w}(s) \tag{2}$$

Referring to Fig. 1,

$$\boldsymbol{u}(s) = H(s)\boldsymbol{y}_v(s) \tag{3}$$

Substitution of Eq. (3) into the first row of Eq. (1) yields the controller input signal $\boldsymbol{y}_v(s)$:

$$\boldsymbol{y}_v(s) = [I - G_{11}(s)H(s)]^{-1}G_{12}(s)\boldsymbol{w}(s) \tag{4}$$

By the use of Eq. (3) again,

$$\boldsymbol{u}(s) = H(s)[I - G_{11}(s)H(s)]^{-1}G_{12}(s)\boldsymbol{w}(s) \tag{5}$$

Finally, when the second row of Eq. (1) is used, it follows that

$$\boldsymbol{z}(s) = \left\{G_{21}(s)H(s)[I - G_{11}(s)H(s)]^{-1}G_{12}(s) + G_{22}(s)\right\}\boldsymbol{w}(s) \tag{6}$$

that gives for the control signal

$$\boldsymbol{u}(s) = H(s)[I - G_{11}(s)H(s)]^{-1}G_{12}(s)\boldsymbol{w}(s) \tag{7}$$

In the present work, the buffet conditions presented in Table 1 were represented.

System Identification

During the open-loop tests in September 1997, the standard technique of measuring system transfer functions by energizing each drive system (shaker and actuator groups) independently and measuring the sensor response provided unexpected results. These were ascribed to the internal damping of the large electrodynamic shaker changing the stiffness of the fin when not energized (a node was artificially forced at the shaker attachment point). Unfortunately, the magnitude of this damping was large compared to the singular

Presented as Paper 99-1317 at the AIAA/ASME/AHS/ASC 40th Structures, Structural Dynamics, and Materials Conference, St. Louis, MO, 12–15 April 1999; received 13 December 1999; revision received 12 January 2001; accepted for publication 17 January 2001.

*Associate Professor. Department of Mechanical and Aerospace Engineering. Senior Member AIAA.
†Head, Aeroacoustics and Structural Dynamics Group, Institute for Aerospace Research. Senior Member AIAA.
‡Principal Research Scientist, P.O. Box 4331, Airframe and Engines Division.
§Aerospace Technologist. Aeroelasticity Branch. Member AIAA.
¶Aerospace Engineer.

Table 1 Buffet conditions

FC	Angle of attack, deg	Dynamic pressure, 10^3 Pa
FCI	12–16	10.8–14.4
FC3	20–24	10.8–14.4
FC5[a]	28–32	14.4–16.8
FC6[b]	28–32	14.4–16.8

[a]Maximum power to shaker: 50%.
[b]Maximum power to shaker: 100%.

effect of each actuator string thereby effectively masking the true transfer function. A solution to this problem was found by feeding all three input variables (actuator groups G1 and G2 and the buffet disturbance) using three simultaneous and independent random processes. However, this procedure slowed down the convergence of the transfer functions due to the increasing importance of the cross talk amongst drivers and transducers. Because the shaker controller could only run relatively short time sequences, an unsatisfactory number of ensembles could be taken to determine the individual transfer functions. Therefore, optimization techniques were required for obtaining the best estimate of the required transfer functions in a least-square sense in terms of the cross- and power-spectral densities measured between a given input and the correspondent output. For every transducer, three transfer functions were found corresponding to the two controls and the one load reference signal. System identification routines were written to determine pole-zero and state-space models from these estimates of the various transfer functions.

Performance Calculations

The power spectral density (PSD) of the disturbance was a known input obtained from the flight tests. Because of hardware limitations, these PSDs were band limited. The frequency content lying outside of each one of the critical modes for buffeting was cut off. Furthermore, in the ground test, this PSD described the shaker input signal that excited the structure at a single point. Also, between the shaker and the structure there was a load cell. The PSD of the output of this load cell was assumed to correspond to the disturbance load applied to the fin to simulate buffeting. The subsequent use of the product between Eqs. (2), (5), and (7) and their respective complex conjugates produced the PSDs of the performance sensors in the open- and closed-loop cases and the control signal, respectively,

$$\mathrm{PSD}_{\mathrm{output}} = |\text{transfer function}|^2 \mathrm{PSD}_{\mathrm{input}} \tag{8}$$

From these PSDs, both the control effort rms values of each actuator group (as a fraction of the maximum allowed by the hardware) and the ratio (closed over open loop) of the rms values of the performance sensors were obtained.

Experimental Setup

The piezoelectric actuation devices were attached to both sides of the starboard vertical fin (Fig. 2). Two banks of amplifiers drove the two groups of actuators acting in opposite phase at each side of the fin to generate bending. The amplifiers fed the maximum voltage differential allowed across the piezoelectric devices (approximately 1500 V peak to peak). The third input signal was given by the 5000-lbf electromagnetic shaker attached to a single point at center of the starboard side of the fin through a load cell, used to monitor the actual dynamic loads transmitted to the structure. Representative buffet time sequences associated with the chosen flight conditions were fed into the computer that controlled the shaker.

Four accelerometers and six strain gauge rosettes situated at strategic points of the fin provided the output signals.

In the control room, an eight-channel data acquisition system was used to acquire real-time frequency-domain data including transfer functions and auto spectra. In addition, a 16-channel digital tape recorder was used to record data from all available signals for subsequent off-line analyses. The signal from two channels could be selected for feedback control through the computer-driven digital signal processing board AT-DSP2200 using a sampling rate of 5 kHz.

Table 2 Feedback control synthesis

Sensor identification	Approximate sensor position	CL identification
A1	Fin tip, near leading edge	CL1
A2	Fin tip, near trailing edge	CL1 and CL2
A3	$\frac{1}{3}$ Span, near leading edge	None
A4	$\frac{1}{3}$ Span, near rudder leading edge	None
SG3	Fin root, near rudder leading edge (critical point)	CL2 and CL3
SG5	$\frac{2}{3}$ Span, near rudder leading edge	CL3

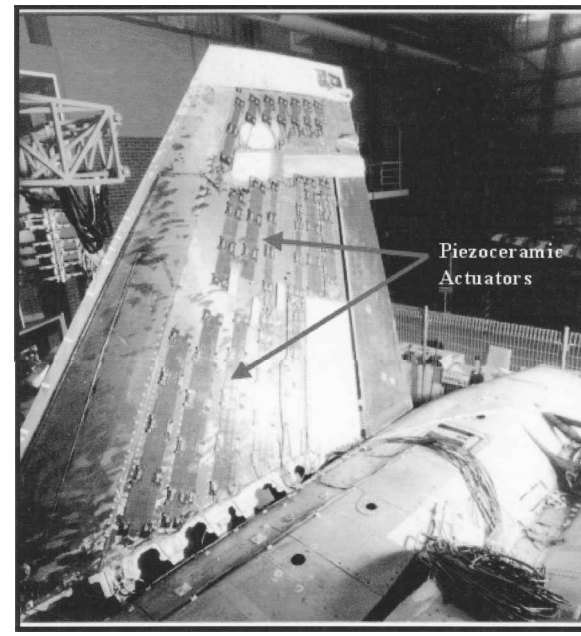

Fig. 2 Instrumented vertical fin.

Parametric Study Involving Sensors

To study the effect that the choice of sensors (strain gauges and/or accelerometers) and sensor location has on the overall performance of the active control system, a parametric study was conducted. It was expected that strain gauges having direct correlation with the system performance metrics would provide better performance. Therefore, three control laws (CL), CL1, CL2, and CL3, were designed based on open-loop test data using the feedback from different pairs of sensors. The identification of the sensors used and their respective participation in a determined control law are summarized in Table 2.

The typical regulator was designed for performance in the bandwidth defined by 10 and 60 Hz, with rolloff at the lower and higher frequencies. The separation theorem of the classic linear quadratic estimator–linear quadratic regulator optimal control theory was used to obtain the Kalman filter and the full-state feedback gains. Emphasis in the control law synthesis was given to attenuate the dynamic response associated with both the first and second natural modes of the vertical fin. All control laws were designed based on open-loop test data for flight condition 1 (FC1).

A bandpass filter was appended in series to the controller output in some designs to cut either a dc signal (when strain is used for feedback) or an undesirable high-frequency response (to guarantee stability).

Experimental Results

Table 3 shows the control performance in the frequency intervals shown. The given bands include modes 1, 2, and 1 and 2 together, respectively. In Table 3, the results for two selected performance metrics are listed: accelerometer 2 (A2) and strain gauge 3 (SG3). From the sensor locations, one can observe that SG3 represented a good measurement of mode 1, whereas A2 was more related to mode 2. All of the three control laws studied presented reduction in the vibration levels associated with mode 1 less significant than

Table 3 Parametric study involving sensors: experimental and theoretical results, ratio of closed- over open-loop rms values (%)

Frequency band, Hz	CL1		CL2		CL3	
	A2	SG3	A2	SG3	A2	SG3
			FC1			
5–25	97.1 (98.2)[a]	99.7 (99.3)	70.3 (71.7)	69.4 (75.9)	64.8 (68.2)	70.0 (74.5)
25–100	82.6 (81.6)	92.6 (87.5)	57.8 (53.0)	42.5 (42.0)	84.9 (86.2)	67.2 (72.8)
5–100	83.3 (82.3)	98.8 (97.7)	58.5 (53.9)	66.7 (72.0)	84.9 (85.5)	69.6 (74.2)
			FC3			
5–25	97.0 (97.0)	98.0 (98.9)	93.3 (93.4)	91.7 (94.0)	92.4 (95.9)	93.0 (95.0)
25–100	81.8 (79.6)	90.0 (92.2)	86.9 (86.2)	82.0 (79.9)	94.1 (95.6)	87.6 (86.5)
5–100	83.1 (81.1)	97.6 (98.5)	87.3 (86.7)	91.3 (93.3)	93.9 (95.6)	92.8 (94.5)
			FC5			
5–25	98.0 (99.5)	98.0 (99.9)	92.3 (93.4)	91.7 (94.0)	93.0 (92.5)	92.6 (96.2)
25–100	88.0 (88.7)	95.3 (94.4)	86.9 (86.2)	82.0 (79.9)	98.2 (95.1)	92.4 (88.5)
5–100	88.3 (89.1)	97.7 (99.3)	87.3 (86.7)	91.3 (93.3)	98.0 (95.0)	92.6 (95.4)

[a](Expected values).

those obtained for mode 2. The best results were obtained when the signal from SG3 was used in the feedback loop, as in case of CL2 and CL3, confirming the initial predictions. Note that CL1 was in the case of FC1 limited in gain to guarantee the controller stability.

The most severe, FC6 was the last to be tested. Because of the accumulative fatigue of the hardware (piezoelectric elements), several attempts to close the loop with the MIMO controller were unsuccessful. During each attempt, an actuator on the upper group failed, resulting in a system automatic shutdown. The apparent reason was the proximity of these actuators to the most stressed region of the fin, near the load cell. Therefore, a single input/single output (SISO) controller was designed for commanding only the lower group of actuators to reduce buffeting in the first bending mode of the tail during a closed-loop run at FC6. When feedback from accelerometer A2 and a nominal gain setting to increase chances of success were used, this SISO controller reduced the rms strain at SG3 by approximately 3% in the frequency range of 10–20 Hz. Between 0 and 100 Hz, the rms strain at SG3 was reduced by approximately 2.5%.

Conclusions

A full-scale aircraft instrumented to reduce buffet loads was tested. The test represents an important step in the development of adaptive smart structures systems. Two groups of actuators consisting of piezoelectric elements distributed over the structure were designed to achieve authority over the first and second modes of the vertical fin.

Very promising results were obtained in parametric studies using different sensors in a two input/two output controller using the standard time-invariant linear quadratic Gaussian control law design. Based on the most important performance metric, the strain gauge located at the critical point for fatigue, vertical fin buffet attenuation of 57.5% (mode 2) and 33.3% (modes 1 and 2) for the nominal FC were observed during the tests. Also, attenuation of 18.3% (mode 2) and 8.7% (modes 1 and 2) were verified for the next most severe buffeting case. In general, the CL that included at least one strain gauge in the feedback loop revealed better performance. This is an indication that strain gauges can be better correlated to the control objective, which is to reduce the structural strain generated by buffeting.

References

[1]Zimmerman, N. H., Ferman, M. A., Yurkovich, R. N., and Gerstenkorn, G., "Prediction of Tail Buffet Loads for Design Application," *Proceedings of the AIAA/ASME/ASCE/AHS/ASC 30th Structures, Structural Dynamics and Materials Conference*, AIAA, Washington, DC, 1989, pp. 1911–1919.

[2]Ferman, M. A., Patel, S. R., Zimmerman, N. H., and Gerstenkorn, G., "A Unified Approach to Buffet Response of Fighter Aircraft Empennage," *Aircraft Dynamic Loads Due to Flow Separation*, CP-483, AGARD, 1990, pp. 2.1–2.18.

[3]Lee, B. H. K., Brown, D., Zgela, M., and Poirel, D., "Wind Tunnel and Flight Tests of Tail Buffet on the CF-18 Aircraft," *Aircraft Dynamic Loads Due to Flow Separation*, CP-483, AGARD, 1990, pp. 1.1–1.26.

[4]Edwards, J. W., "Unsteady Airloads Due to Separated Flow on Airfoils and Wings," *Aircraft Dynamic Loads Due to Flow Separation*, CP-483, AGARD, 1990, pp. 16.1–16.18.

[5]Rock, S. M., Ashley, H., Digumarthi, R., and Chaney, K., "Active Control for Fin Buffet Alleviation," *Proceedings of Advances in Aerospace Sciences: A Tribute to Prof. Holt Ashley*, Stanford Univ. Press, Stanford, CA, 1993, pp. 413–421.

[6]Nitzsche, F., Zimcik, D. G., and Langille, K., "Active Control of Vertical Fin Buffeting with Aerodynamic Control Surface and Strain Actuation," *Proceedings of the AIAA/ASME/AHS Adaptive Structures Forum*, AIAA, Washington, DC, 1997, pp. 1467–1477.

[7]Moses, R. W., "Vertical Tail Buffeting Alleviation Using Piezoelectric Actuators," *Proceedings of SPIE 4th Annual International Symposium on Smart Structures and Materials, Industrial and Commercial Applications of Smart Structures Technologies*, Vol. 3044, Society of Photo-Optical Instrumentation Engineers, Bellingham, WA, 1997.

Digital Redesign of Linear State-Feedback Law via Principle of Equivalent Areas

Tohru Ieko*
Japan Defense Agency, Meguro, Tokyo 153-8630, Japan
and
Yoshimasa Ochi† and Kimio Kanai‡
National Defense Academy, Yokosuka, Kanagawa 239-8686, Japan

Introduction

DIGITAL redesign is an approach to design of a discrete-time (DT) controller via conversion of a continuous-time (CT) controller. There are some advantages of the digital redesign: First, a lot of design methods are available for CT controller design. Second, the behavior of CT systems can be physically more easily understood, which makes analysis and synthesis of CT control systems simpler without being bothered with selection of sampling periods. Third, changing the sampling period does not require total redesign of the control system, but just requires conversion of the CT controller for a new sampling period. In addition, intersampling behavior, which is sometimes overlooked in the direct DT controller design, can be taken into account. Particularly, digital redesign methods that preserve the closed-loop characteristics of the original CT control systems[1–7] are more effective for larger sampling periods than open-loop redesign methods such as Tustin's (see Ref. 8). We proposed a closed-loop digital redesign method for one-degree-of-freedom dynamic compensators[7] based on the principle of equivalent areas (PEA).[9] In this Note, we present a digital redesign method for a linear state-feedback control law also based on the PEA. That is, the DT input is determined so that the integral of the closed-loop CT

Received 14 March 2000; revision received 16 February 2001; accepted for publication 26 February 2001.

*Major, Japan Ground Self Defense Force, Technical Research and Development Institute, 2-2-1 Nakameguro.

†Associate Professor, Department of Aerospace Engineering, 1-10-20 Hashirimizu. Senior Member AIAA.

‡Professor, Department of Aerospace Engineering, 1-10-20 Hashirimizu. Associate Fellow AIAA.